The Gastrointestinal System

Giovanna Bertolini

1 Introduction

The increased temporal and spatial resolution of most modern MDCT scanners enables routine examination of the gastrointestinal tract in small animals. The veterinary literature on this topic is in its infancy, but recent papers have shown the usefulness of contrast-enhanced 16-MDCT as a preliminary screening modality in awake or minimally sedated dogs with acute abdominal signs, including gastro-intestinal obstruction and perforation. In patients with neoplastic and nonneoplastic obstructive diseases, MDCT can be used to identify the affected segment and, in most cases, the cause of obstruction. In neoplastic conditions, MDCT is essential for staging and aids intervention planning.

2 MDCT Imaging Strategies

No common strategy for gastrointestinal MDCT has been established for veterinary patients. Patient preparation and scanning protocols can vary, depending on the suspected pathology. At our center, gastrointestinal CT examinations are generally performed with anesthetized patient. This allows performing endoscopy and bioptic procedures under the same anesthesiology episode. In general, adequate distension of the gastrointestinal tract is necessary for the evaluation of wall thickness and integrity, as collapsed intestinal segments can falsely show wall thickening and non-distended gastric plication may conceal small gastric ulcerations. The use of helical hydro-CT for better characterization of gastric tumors has been described in

G. Bertolini (✉)
San Marco Veterinary Clinic, Padua, Italy
e-mail: bertolini@sanmarcovet.it

dogs with single-slice CT. The recommended dose of water is 30 mL/kg, and the hydro-CT study should be followed by intravenous contrast medium (CM) administration. The use of air/gas contrast is more appropriate with MDCT scanners than the use of water or other neutral fluids, as it allows the acquisition of endoluminal through-flight images from the same volume dataset. In patients with suspected gastrointestinal hemorrhage (i.e., those with hematemesis), no oral CM should be administered; positive CM may mask bleeding, and water or another neutral CM may dilute the extravasated intravenous CM, thereby compromising the ability to identify the site of bleeding. In post-contrast series, moreover, positive oral CM prevents evaluation of the mucosal pattern of enhancement.

Most advanced MDCT scanners can acquire thin-collimated, near-isotropic, or true-isotropic imaging data for the gastrointestinal tract. Multiplanar and 3D views, including endoluminal imaging, can provide detailed information about various pathological conditions. Acquisition of a pre-contrast series is recommended in patients with suspected gastrointestinal hemorrhage. Post-contrast series should include the (late arterial phase) LAP and (portal venous phase) PVP. Properly timed CM injection can reveal even small lesions and subtle changes in mucosal contrast enhancement. In the LAP (or inflow portal phase), the gastrointestinal mucosa shows maximum
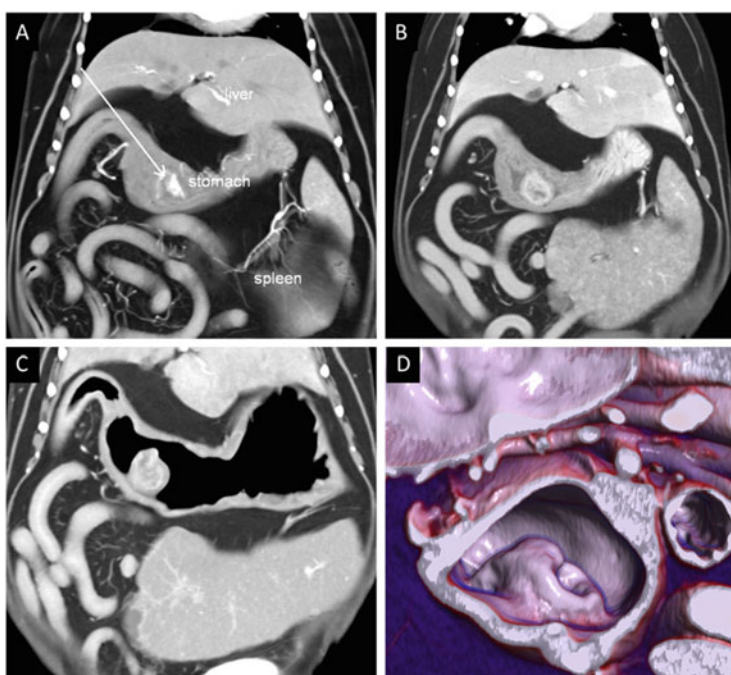
Fig. 1 Multiphasic study in a dog with a gastric mass (leiomyosarcoma). (**a**) Dorsal MPR view of the abdomen (thin slab average) in the HAP. *Arrow* indicates the site of active hemorrhage. (**b**) PVP image from the same dog, with a non-distended stomach. (**c**) Dorsal view obtained after gas insufflation (equilibrium phase). The dimensions and margins of the mass are more appreciable. (**d**) 3D segmentation of the same volume dataset, showing the characteristics of the mass, including large and deep ulceration

enhancement. The arterial phase may show active hemorrhage in patients with benign or malignant gastrointestinal ulceration (Fig. 1). In patients with gastrointestinal tumors, both vascular phases add useful information regarding the vascularity of the mass and the metastasis of lesions to the liver, generally detected in the PVP.

3 Gastrointestinal Thickening

The normal stomach wall thickness is related to the degree of gastric distention, and rugal folds tend to disappear when the stomach is distended. Focal or diffuse gastric wall thickening can be found with inflammatory disease or infiltrative neoplasia, and significant overlap exists between in the imaging features of the two conditions. Gastric wall thickening and thickened folds are common CT sign of gastritis in dogs. Inflammatory polypoid or mass-like folds are difficult to distinguish from gastric lymphoma or other tumors (Figs. 2, 3, 4, and 5).

It has been demonstrated that small intestinal wall thickness varies with weight in the dog, and the duodenal wall is always thicker than the jejunum. In both dogs and cats, the colon wall is generally thinner than the adjacent small intestine, especially when the colon is distended. The gastrointestinal diameter (serosa to serosa) and wall thickness (serosa to mucosa) have been assessed in the non-distended bowels of dogs using single-slice CT. The results (Fig. 6) were

Fig. 2 Gastric rugal fold thickening (chronic lymphoplasmacellular gastroenteritis) in a dog that was referred to our center for suspected gastric neoplasia. Note the conspicuous gastric folds, showing greater enhancement, particularly evident at the gastric fundus. Note also the moderate enlargement of a gastric lymph node (LN), which is normally barely visible
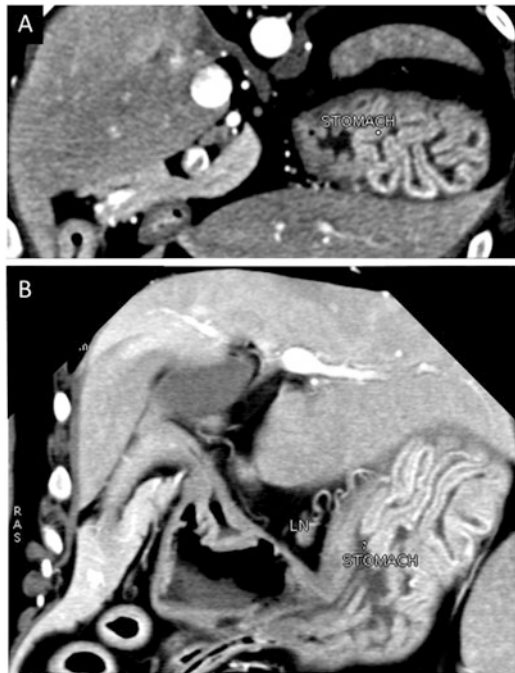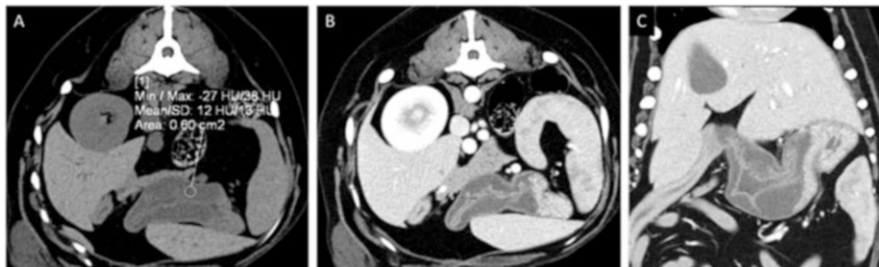
Fig. 3 Gastric wall thickening in a dog with acute gastritis. (**a**) Non-contrast image showing submucosal hypoattenuation at the pyloric antrum and canal, consistent with gastric submucosal edema (12 HU). (**b**, **c**) Transverse and dorsal MPR views of the same dog
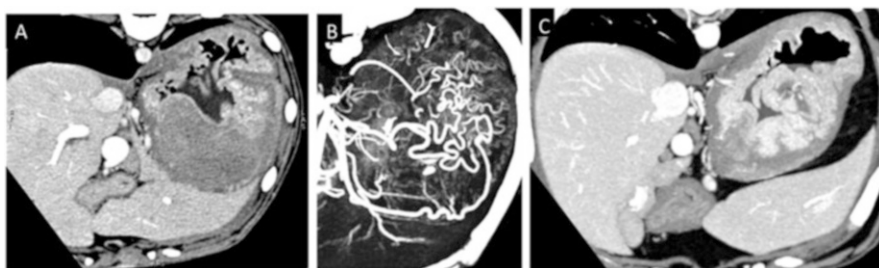
Fig. 4 Gastric wall thickening. (**a**) Transverse view (PVP). Massive mural thickening at the body of the stomach in a dog with aspergillosis. (**b**) MIP view from the HAP showing increased and tortuous arterial vasculature of the stomach due to inflammation. (**c**) CT monitoring image obtained 8 months later. The gastric wall is less thickened and the gastric folds are noticeable, mimicking a mass in the non-distended stomach
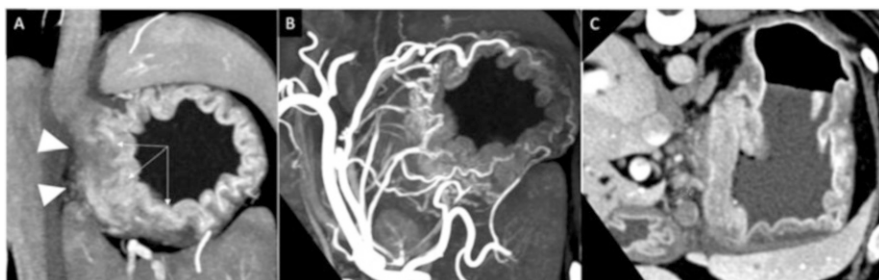
Fig. 5 Gastric wall thickening (gastric carcinoma). (**a**) Dorsal thin-MIP view of the stomach. Note the irregular gastric wall thickening at the lesser curvature (*arrows*). The outer border of the tumor is irregular (*arrowheads*). (**b**) Dorsal MIP from the LAP, showing the blood supply to the neoplastic wall. (**c**) Note the perilesional fat thickening and regional lymph node enlargement

similar to those reported for radiology and ultrasound, which remains the first-line imaging modality for the evaluation of diffuse gastrointestinal disease in small animals. Focal or diffuse gastrointestinal thickening is encountered frequently in veterinary patients, has many causes, and is easily documented by MDCT. As has

Gastrointestinal Regions	Wall thickness (mm)	Segment diameter (mm)
Stomach (fundus, body, pylorus)	0.98 – 2.13 (<9kg); 2 – 3.55	
Pyloric antrum	1.69 -2.74 (<9kg) ; 2.95 – 4.40	9.69 – 12 (<9kg); 13.54 – 16.16
Ascending duodenum	2.59 – 3.30 (< 9 Kg); 4.61 – 5.26	
Descending duodenum		8.79 – 10.46 (<9kg); 11.60 – 16.63
Jejunum	2 – 2.93 (<9kg); 3.31 – 3.87	6.95 – 8.21 (<9kg); 9 – 12.53
Ascending colon	1.05 – 1.45 (<9kg); 1.78 – 2.35	
Transverse colon		9 – 11.93 (<9kg); 12.84 – 21.49

Fig. 6 Wall thickness and segment diameter for various gastrointestinal regions (related to body weight), determined in a group of dogs using a single helical CT unit (Hoey et al. 2013; see the full reference at the end of the chapter)

been said for the stomach, many benign and malignant diseases can lead to gastrointestinal thickening, and considerable overlap exists in the appearance of inflammatory and neoplastic diseases (Figs. 7, 8 and 9). The patient's history and clinical signs are essential in the differential diagnosis. Imaging-guided aspiration, endoscopy, or full thickness biopsies remain necessary for further definition.

4 Gastroduodenal Erosions and Ulcerations

Erosion refers to a defect of the gastric or duodenal mucosa, whereas gastroduodenal ulceration refers to a defect that penetrates the muscularis mucosa. Gastroduodenal ulcerations may develop as the consequence of excessive acid, pepsin, or other harmful substance; they can occur independently or as a complication of many systemic diseases and medical treatments. Inflammatory conditions (gastroenteritis) and the use of steroids and nonsteroidal anti-inflammatory drugs are probably the most common causes of gastrointestinal erosion and ulceration in veterinary patients. Anti-inflammatory drugs decrease local prostaglandin production, thereby reducing mucosal blood flow and limiting the epithelium's capacity to protect itself from the injurious effects of gastric acid. Many other diseases (e.g., mast cell tumor, gastrinoma) are associated with increases in histamine and gastrin levels, which increase gastric acid production, leading to gastrointestinal erosion and ulceration.
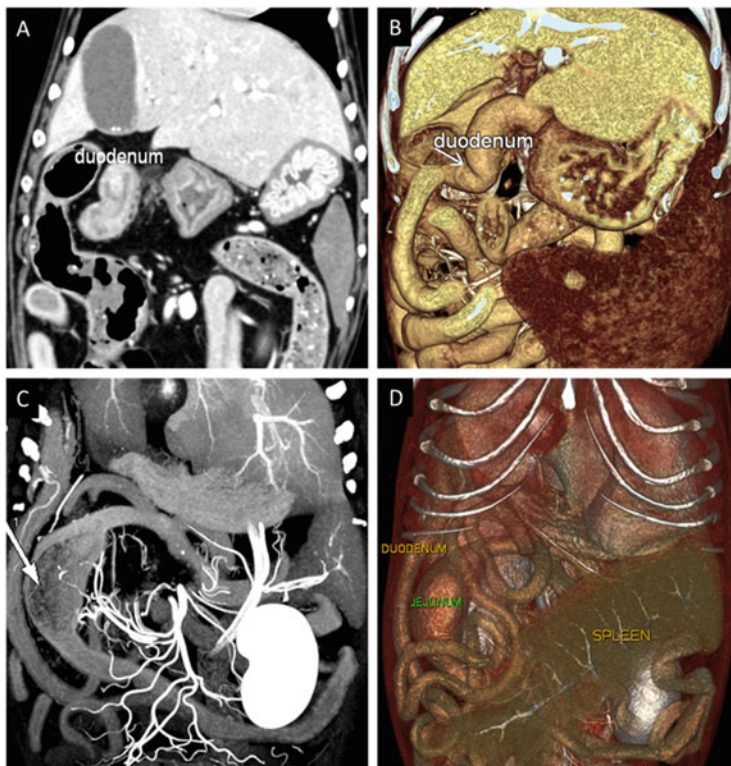
Fig. 7 Intestinal wall thickening. (**a**) Dorsal MPR view of the abdomen in a dog with lymphocytic-plasmacytic enteritis. (**b**) Volume-rendered image of the abdomen in the same dog. Note the diffuse thickening of the intestinal loops. *S* spleen; note a small hypervascular lesion (extramedullary hematopoiesis). (**c**, **d**) Dorsal MIP and volume-rendered images of a dog with segmental jejunal dilatation and focal enteritis due to a subocclusive plastic foreign body (rubber pacifier)

MDCT of *erosion and gastroduodenal ulceration* in small animals has not been described to date. Many MDCT characteristics of gastroduodenal ulceration reported in humans may be observed also in dogs and cats with this condition, with the appropriate use of advanced MDCT technology. Direct and indirect MDCT signs may be encountered in veterinary patients. The disruption of mucosal enhancement (in the LAP) and focal luminal outpouching (ulcer crater development) are the most common direct CT signs of ulceration associated with benign and malignant conditions (Figs. 10, 11, 12, and 13). Indirect signs of erosion or gastric ulceration include gastric fold thickening, mucosal hyperenhancement, and perigastric/periduodenal inflammation (e.g., increased opacity of fat with hazy/ground-glass-like appearance, presence of fluid film). In complicated cases, other CT signs may be present. Complications of gastroduodenal ulceration include active hemorrhage and perforation. Active hemorrhage may not be noted unless a
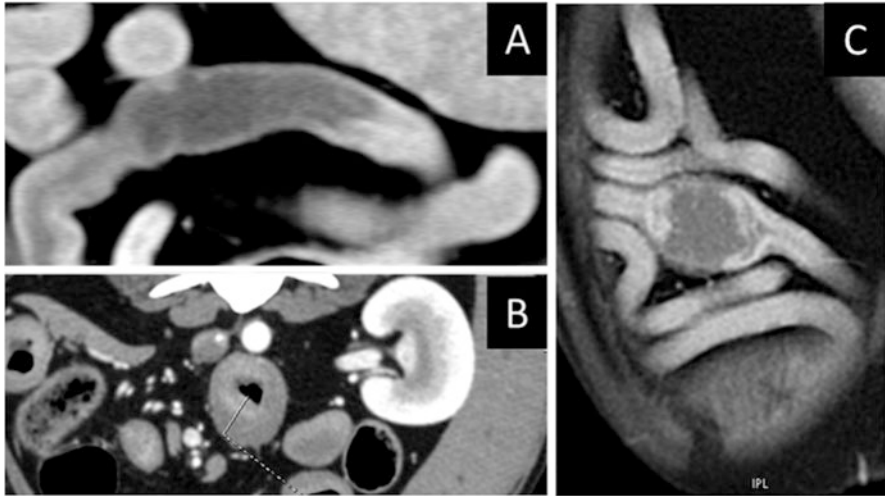
Fig. 8 Focal intestinal thickening. (**a**) Segmental jejunal thickening in a dog with lymphocytic-plasmacytic enteritis. (**b**) Transverse view from a dog (20 kg) with eccentric jejunal segmental thickening (serosa-mucosa diameter, 14 mm), resulting in lymphoma. (**c**) Jejunal focal thickening in a dog with intestinal hemangiosarcoma
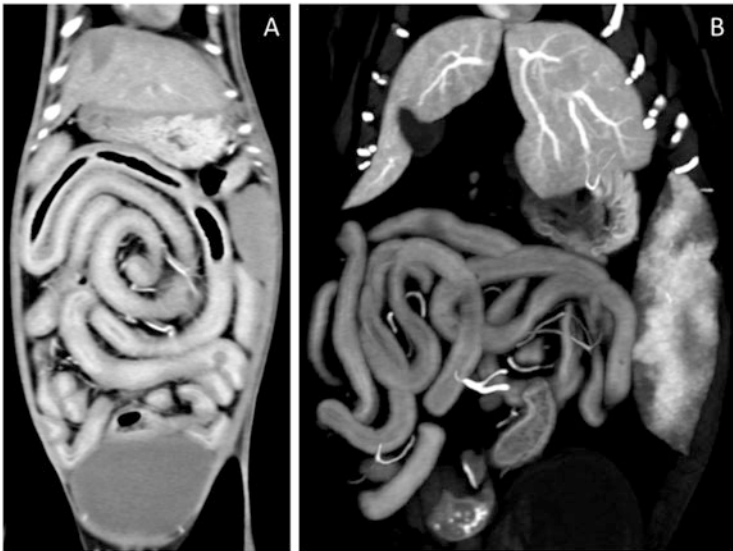

Fig. 9 Diffuse intestinal thickening in two cats with lymphoma

tailored protocol is performed. Direct scans may or may not reveal hyperattenuating material, especially in cases of intermittent bleeding. In the detection of active bleeding with CTA, the greatest sensitivity is achieved by combining findings from the arterial phase and PVP. CM extravasation is observed during the arterial phase,
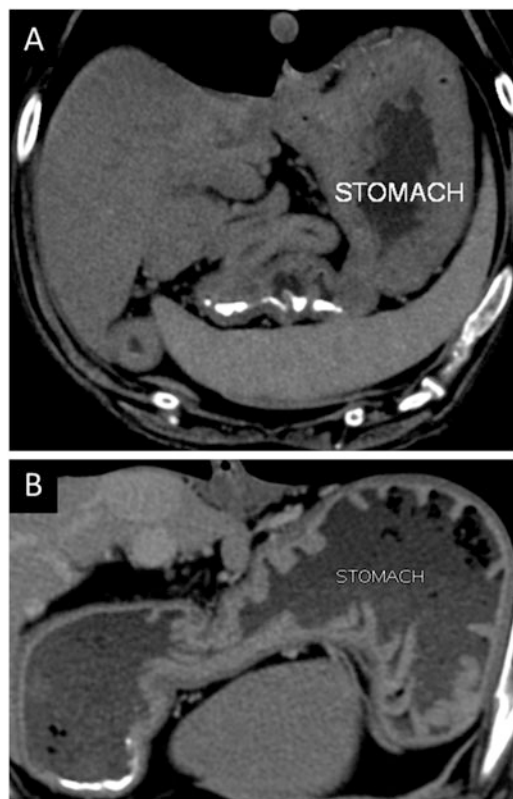
Fig. 10 Gastric erosion. (**a**) Non-contrast transverse view of the stomach in a dog with intestinal sarcoma (not visible here). Note the hyperattenuating material on the gastric mucosal surface, corresponding to ulcerative areas with hemorrhage on endoscopic evaluation. (**b**) Hemorrhagic gastric erosion in a dog due to FANS (nonsteroidal anti-inflammatory drug) therapy
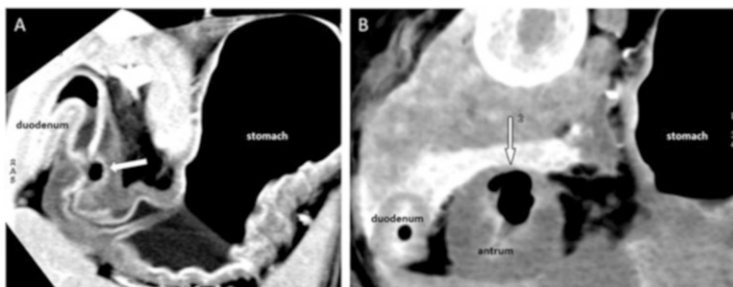
Fig. 11 Ulceration of the stomach in a dog after FANS (nonsteroidal anti-inflammatory drug) overdose. (**a**) Dorsal MPR view. The stomach is distended by gas and fluid. The pyloric antrum shows wall thickening and mucosal interruption, with focal gas collection (*arrow*). (**b**) Transverse MinIP view showing the gas collection expanding into the submucosa. Endoscopic examination confirmed the gastropathy with ulceration
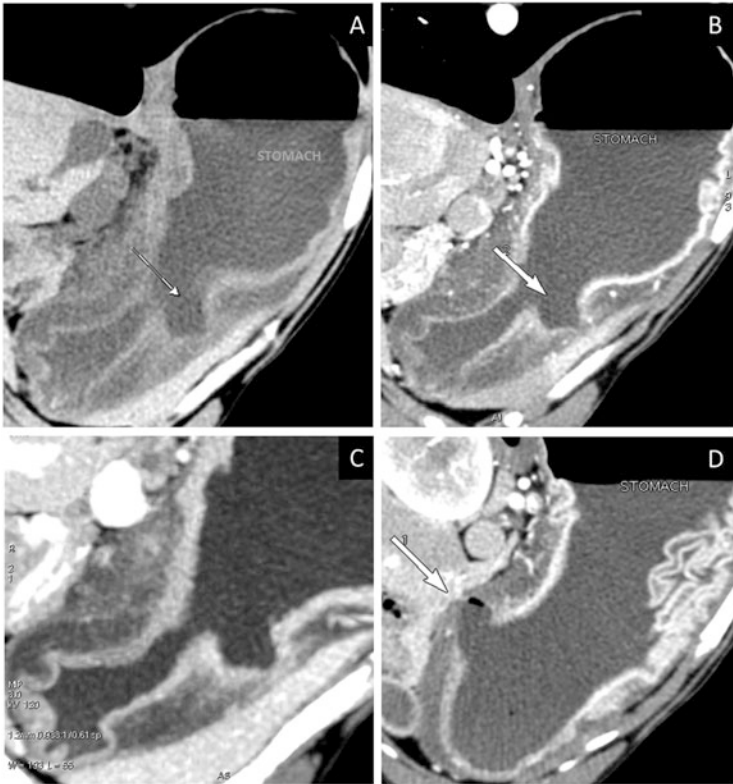
Fig. 12 Complication of a benign ulcer. (**a**) Pre-contrast transverse image of the stomach in a dog with lymphocytic-plasmacytic gastroenteritis. Note the thickened gastric wall. *Arrow* indicates a deep ulcer of the gastric body, with pronounced border having regular margins. (**b**) Same image from the LAP showing the intact mucosal layer. (**c**) MIP from the PVP showing the intact mucosal layer. (**d**) In the same dog, another gastric ulcer at the small curvature, showing interruption of the mucosal layer and the presence of a small gas bubble. These signs are consistent with a perforated ulcer (confirmed by endoscopic examination)

and CM pooling/accumulation is visible during the PVP (Fig. 14). Pre-contrast and dual-phase MDCT of the abdomen should always be performed in patients with histories of hematemesis or hematochezia or laboratory signs of gastrointestinal bleeding.

5 Gastrointestinal Perforation

Gastrointestinal perforation can have various causes in veterinary patients. Most perforations are emergency conditions of the abdomen that require early recognition and timely surgical treatment. Gastrointestinal ulcers, necrotic or ulcerated
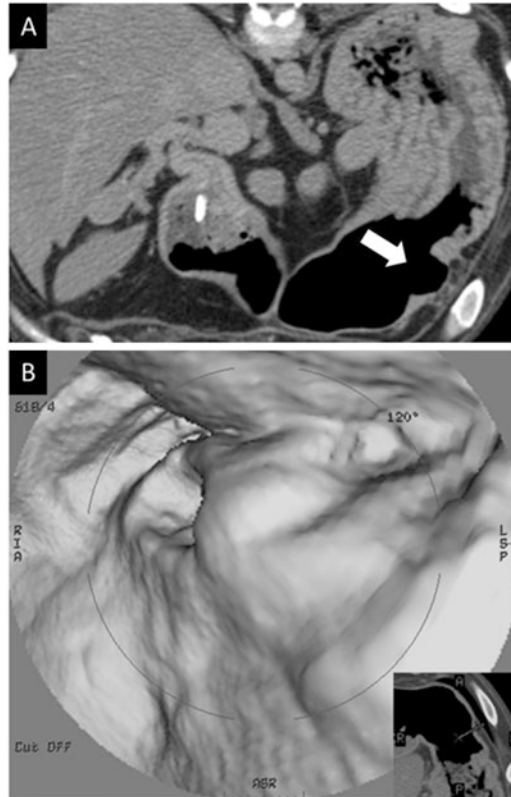
Fig. 13 Malignant gastric ulcer (lymphoma). (**a**) Transverse view of the stomach in a dog showing a profound focal defect at the body of the stomach (*arrow*). (**b**) Endoluminal imaging (virtual endoscopy) of the stomach showed an ulcerative lesion surrounded by prominent, irregular margins
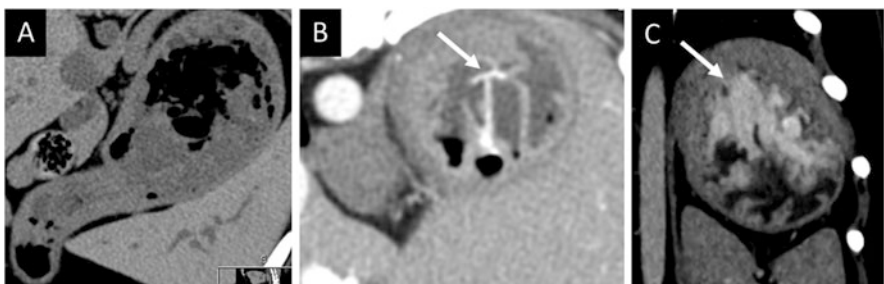

Fig. 14 Active hemorrhage in a dog. (**a**) Pre-contrast image shows no sign of hemorrhage. (**b**) Transverse view from the LAP showing initial extravasation of CM in the stomach (*arrow*). (**c**) CM pooling/accumulation in subsequent scans

malignancies, and iatrogenic and traumatic injuries are the most common causes of GIP. MDCT is very sensitive in GIP detection, and it can also be used to localize the perforation site. In humans, the reported overall accuracy of CT for bowel perforation site prediction ranges from 82 to 90%. The diagnosis of GIP is based on direct and indirect MDCT findings. Direct CT signs are discontinuity of the bowel wall and the presence of extraluminal air. Indirect MDCT findings of GIP include intestinal wall thickening, abnormal wall enhancement, abscess, and the presence of an inflammatory peritoneal mass adjacent to the perforated intestinal segment (Figs. 15 and 16). Depending on the perforation site, free air may be detected in intraperitoneal or retroperitoneal spaces. Gastric and small bowel perforation leads to pneumoperitoneum, whereas large bowel perforation may lead to pneumoretroperitoneum (Fig. 15c). In small bowel perforations, especially when the amount of air is small, concentrated free air bubbles may be seen in close proximity to the intestinal wall. In these cases, MDCT images should be examined thoroughly because free air bubbles tend to stay near the wall from which they arise, and their location may thus aid determination of the perforation site.
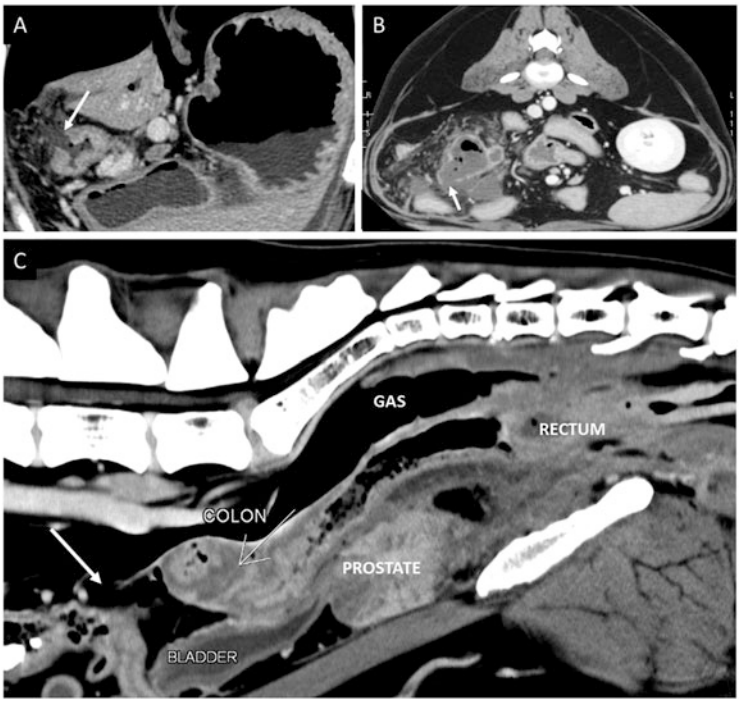

Fig. 15 Intestinal perforation. (**a**) Duodenal perforation in a patient with chronic lymphocytic-plasmacytic enteritis. Note the duodenal discontinuity and intestinal content leakage into the peritoneal cavity (*arrow*). (**b**) Jejunal perforation in a dog with severe mural enteritis. Note the discontinuity of the bowel wall (*arrow*) and surrounding peritoneal thickening and stranding (focal peritonitis). (**c**) Perforation of the descending colon (*arrow*) in a dog with carcinoma, following a biopsy procedure. Note the retropneumoperitoneum (gas)
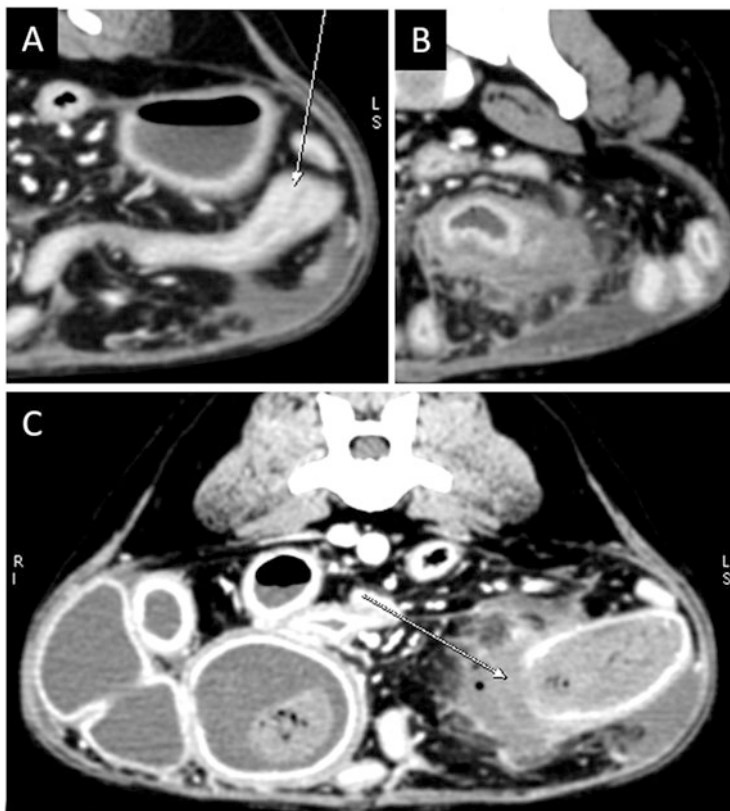
Fig. 16 Intestinal perforation in a dog with obstruction. (**a**) Transverse view of the abdomen showing the narrowing of the jejunal segment. (**b**) Transverse view of the affected segment, showing the thickened intestinal wall and the perilesional peritoneal mass (abscess) adjacent to the perforation site. Note the presence of free fluid in the peritoneal cavity. (**c**) Other intestinal segments are distended by fluid. Note the ruptured intestinal wall (*arrow*), perilesional fluid, and peritoneal thickening and stranding. Surgery confirmed stenosis and prestenotic dilatation and intestinal rupture. Histopathology proved fibrinous purulent enteritis and septic peritonitis

6   Gastrointestinal Obstruction

Gastric outlet obstruction may occur in association with congenital and acquired conditions. Pyloric stenosis refers to congenital benign muscular hypertrophy of the pylorus and is seen in young brachycephalic dogs and Siamese cat. Acquired conditions (e.g., foreign bodies, masses, or infiltrative diseases) can cause hypertrophy of the antral mucosa or a combination of both muscular and mucosal thickening (e.g., chronic hypertrophic pyloric gastropathy) (Figs. 17 and 18). Other nonneoplastic conditions leading to gastric outlet obstruction include intussusception and herniation (hernias are treated in the Chapter "The Peritoneal
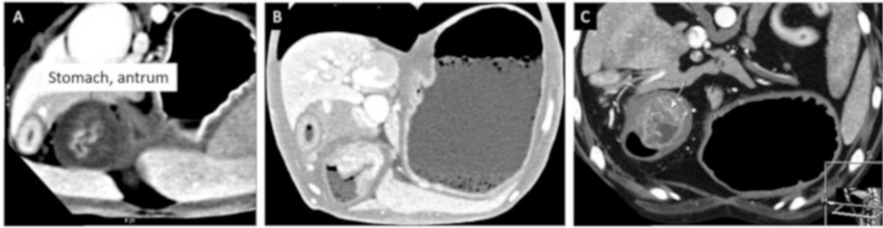
Fig. 17 Pyloric outflow obstruction. (**a**) Benign muscular hypertrophy of the pylorus (congenital pyloric stenosis) in a young bulldog. Note the smooth circumferential pyloric wall thickening involving the muscular component. The mucosa has a normal appearance. The stomach shows moderate dilatation by gas. (**b**) Benign hypertrophy of the pyloric mucosa (chronic antral mucosal hypertrophy) in a mongrel dog, causing outflow obstruction. Note the dilatation of the stomach, which contains fluids and gas. (**c**) Malignant pyloric obstruction in a dog with gastric sarcoma (*arrow*). The stomach is distended by gas
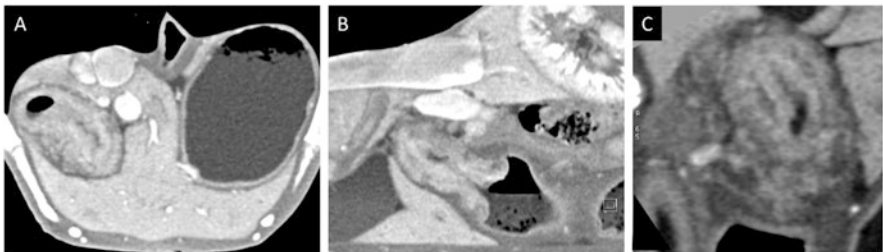
Fig. 18 Malignant hypertrophic pyloric stenosis secondary to gastric carcinoma in a dog. (**a**) Transverse view showing circumferential smooth wall thickening in the antropyloric region of the stomach. The stomach is distended by fluid and gas. (**b**) Midsagittal oblique view showing narrowing and stenosis in the antropyloric region. (**c**) Close-up view of a transverse section of the pyloric region, showing a CT appearance resembling that described in humans (cervix sign, due to indentation of the pylorus into the fluid-filled antrum)

Cavity, Retroperitoneum, and Abdominal Wall"). Intussusception involving the stomach is rarely reported in dogs and cats. A few cases of pylorogastric intussusception have been reported in the veterinary literature to date. Gastro-gastric intussusception not involving the pylorus is also possible (Fig. 19).

Many intrinsic and extrinsic conditions may lead to intestinal narrowing. Common causes of mechanical *small and large bowel obstruction* in dogs and cats are foreign bodies, intussusception, inflammation, neoplasia, abscess, granuloma, and strictures. MDCT examination is generally required in patients with suspected malignant gastrointestinal obstruction or in those with clinical signs of obstruction and unclear results of first-level imaging. In humans, CT evaluation of mechanical intestinal obstruction is highly sensitive, specific, and accurate, allowing identification of the site and cause of obstruction with up to 100% sensitivity. In a recent study, CT outperformed digital radiology in the determination of site and cause of
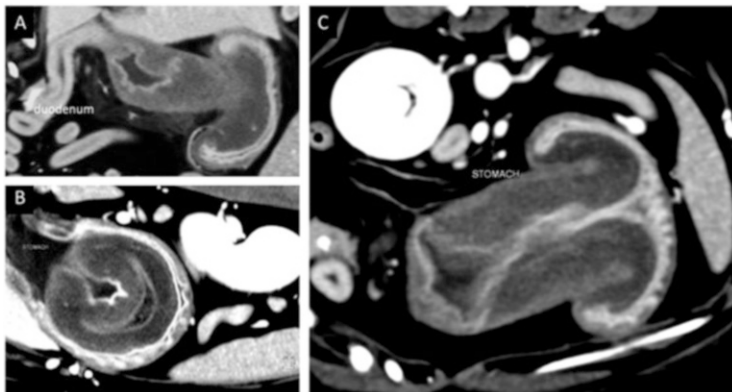
Fig. 19 Gastric outlet obstruction in a young Labrador retriever due to invagination of the antrum into the body of the stomach (gastro-gastric intussusception). (**a**) Note the normal appearance of the pylorus and duodenum, which are not involved in the intussusception. (**b**, **c**) Transverse and sagittal views of the affected part of the stomach

obstruction in 20 dogs, showing greater sensitivity (95.8 vs. 79.2%) and specificity (80.6 vs. 69.4%).

Most CT signs of obstruction reported in humans are encountered also in veterinary patients. Direct CT signs of mechanical intestinal obstruction or strangulation include dilated fluid-filled bowel loops with normal or collapsed distal loops; bowel thickening (mural edema or hemorrhage); U- or C-shaped appearance in cases of volvulus; and hyperattenuation of an intestinal segment on pre-contrast images with absent, reduced, or delayed intestinal wall enhancement on post-contrast images (bowel ischemia or hypoperfusion) (Figs. 20, 21, 22, 23, 24, and 25). Indirect signs include stretched or prominent mesenteric vessels, the "whirl sign" for twisted mesenteric vessels (also seen in torsion of other abdominal organs), and mesenteric fat stranding (Fig. 26). The latter has been described as a feature of mechanical obstruction in dogs, but it is not specific to obstruction and can be found in a broad spectrum of abdominal diseases. However, when detected in patients with suspected gastrointestinal obstruction, it should prompt the examiner to evaluate the regional viscera more rigorously, as it frequently appears adjacent to the obstructed intestinal segment. Other CT signs, such as mesenteric thrombosis and the reticulonodular mesenteric pattern, seen in neoplastic conditions, may accompany mechanical bowel obstruction. Advanced small bowel obstruction leads to bowel dilatation and necrosis or perforation of the intestinal wall (Fig. 16).

Intestinal pseudo-obstruction is a functional disorder of the bowel mimicking clinical and imaging signs of obstruction but in the absence of any mechanical
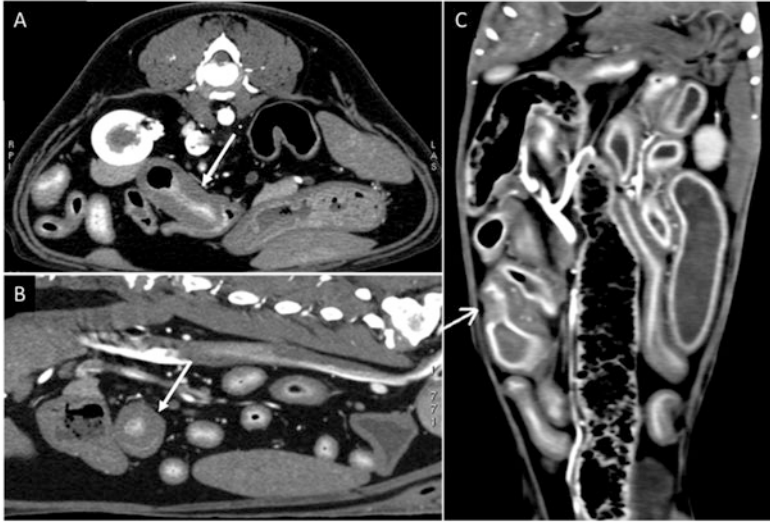
Fig. 20 Intestinal stenosis. (**a**) Ileal narrowing and stenosis in a dog with chronic intestinal inflammatory disease. Transverse view of the abdomen. Moderate prestenotic distention by gas is visible. (**b**) Midsagittal view of the abdomen, showing the transverse section of the affected intestinal segment (*arrow*). (**c**) Jejunal narrowing in a cat with lymphoma (*arrow*). Note the distension of other intestinal loops containing fluid and gas
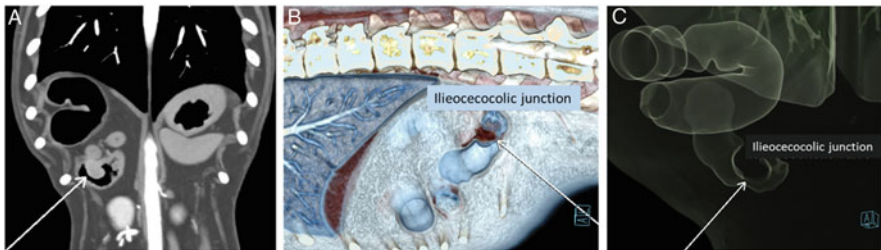
Fig. 21 Partial intestinal stenosis at the ileocococolic junction in a dog due to a polypoid lesion. (**a**) Dorsal MPR view showing a mass-like lesion protruding into the intestinal lumen at the ileocolic junction. (**b**) Thin-VR of the same volume. (**c**) VR of air-content structure of the body of the stomach, showing the site of the mass and prestenotic bowel dilatation

obstruction. The differentiation between true bowel obstruction and pseudo-obstruction may be problematic using only first-line imaging modalities. MDCT may play an important role in the diagnostic workup of pseudo-obstruction, as it can rule out mechanical causes of obstruction (Fig. 27). However, full thickness intestinal biopsies are the only diagnostic procedure that allows the definitive diagnosis.

Fig. 22 Intestinal strangulation. (**a**) Thin-MinIP transverse view of the abdomen in a dog showing intestinal stenosis (*arrow*). Note the opacification of surrounding omental fat and the distention of other areas of the intestinal tract by fluid and gas. (**b**) Parasagittal view in the same dog showing the stenotic intestinal tract, involving the distal jejunum and ileum. (**c**) Dorsal MPR view showing intestinal loop strangulation (*arrow*). (**d**) Thin-average dorsal MPR view which better defines the strangulation and the absence of an endoluminal or extraluminal mass. Based on CT, intestinal strangulation due to an internal hernia was suspected. Surgery confirmed that parts of the jejunum and ileum were incarcerated in an unusual gap in the greater omentum. Intestinal histopathology revealed severe fibrosis and mild lymphocytic-plasmacytic enteritis

7 Gastrointestinal Masses

Primary gastric and small bowel tumors are rare in small animals. Canine gastric cancer is diagnosed rarely and is reported to account for approximately 0.1–0.5% of canine neoplasias. MDCT characteristics of various tumor types have not been
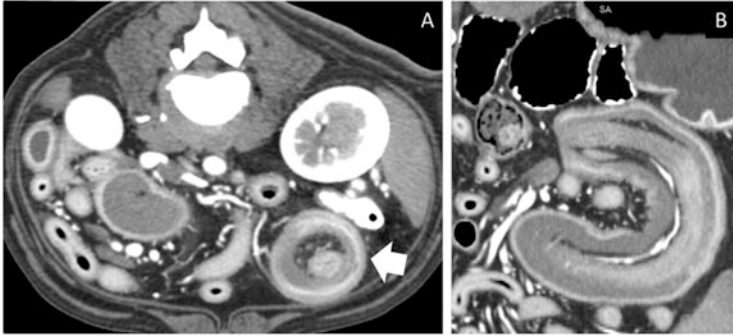
Fig. 23 Intestinal intussusception in dog that underwent CT for staging of hepatic carcinoma. (**a**) Transverse view of the abdomen showing a typical target-shaped lesion resulting from the pulling of the bowel into a neighboring (ileo-jejunal) segment. Note that part of the omentum is also intussuscepted. Other segments are distended by fluid or air. (**b**) Dorsal MPR view showing the multilayered, C- or U-shaped intestinal appearance, the thickened intestinal wall, hypoattenuation due to ischemia, and consequent wall edema. Note the mesenteric vessels inside the intussuscepted segment
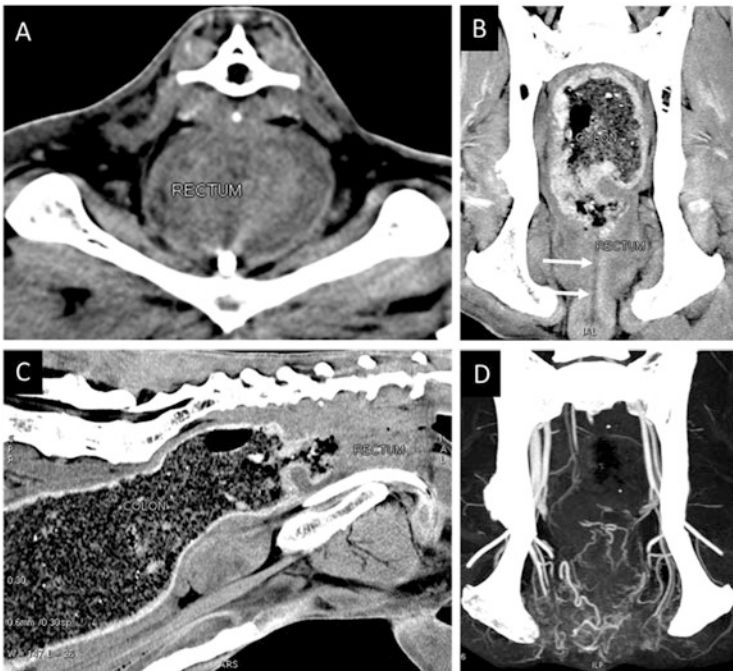
Fig. 24 Benign rectal stenosis due to severe rectal inflammation and proctitis in a German shepherd. (**a**) Pre-contrast transverse image through the pelvis, showing stenosis of the rectum with a mass-like appearance. (**b**) Pre-contrast dorsal MPR view shows a thin, straight hypoattenuating line (*arrows*) indicating the rectal lumen. (**c**) Pre-contrast sagittal view showing stenosis of the rectum and distension of the colon by fecal material. (**d**) Post-contrast dorsal thin-MIP view shows the intense blood supply to the rectal and anal segments due to inflammation
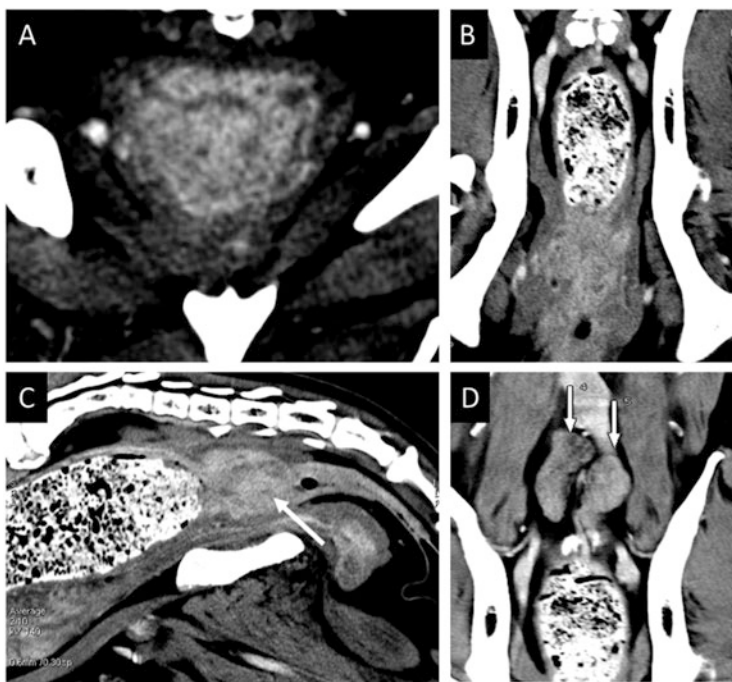
Fig. 25 Malignant stenosis due to colon carcinoma in a dog. (**a**) Transverse view through the pelvis, showing distension and mass-like appearance of the distal part of the descending colon. (**b**) Dorsal MPR view showing moderate contrast enhancement of the colonic mucosa. (**c**) Sagittal view showing a mass obstructing the colon (*arrow*). The rectum is empty and not involved. (**d**) Dorsal MPR view shows only enlargement of the median sacral lymph nodes (*arrows*), resulting in lymph node metastasis

reported in the veterinary literature, and the definitive diagnosis of gastrointestinal tumors is based on cytological or histological demonstration of neoplastic cells.

The main advantage of MDCT over other imaging techniques and endoscopy is that it enables tumor detection and staging during the same procedure. Advanced MDCT scanners can acquire datasets with near-isotropic voxels, with the high resolution needed for diagnostic multiplanar reconstruction and 3D endoluminal imaging. Dorsal, sagittal, and multioblique views of small bowel tumors demonstrate signs of small bowel obstruction, perforation, as well as the mural and extramural extent of small bowel malignancies. Such visualization aids the planning of further diagnostic steps and surgical resection. In addition, regional extent and metastases or peritoneal seeding can be detected with whole-body MDCT.

Benign gastrointestinal tumors (leiomyoma, adenoma) are often discovered incidentally in middle-aged or older patients. Benign gastric tumors may be located submucosally, intramurally, or subserosally and appear on CT as nodular eccentric mural thickening, generally well circumscribed, covered by intact mucosa, with a homogenous appearance and uniform contrast enhancement (Fig. 28). Carcinomas
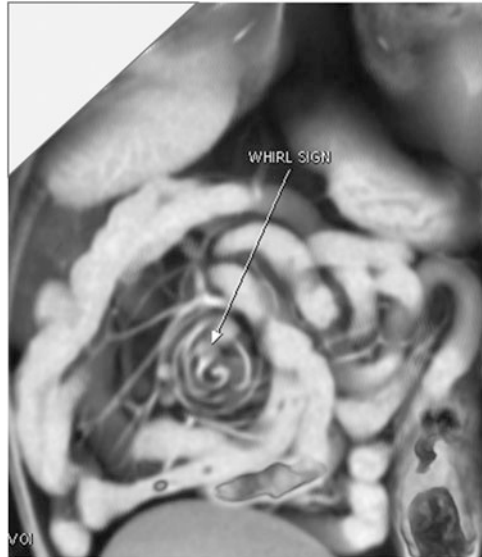
Fig. 26 The "whirl sign" (twisting of the mesenteric vessels) in a cat with lymphoma
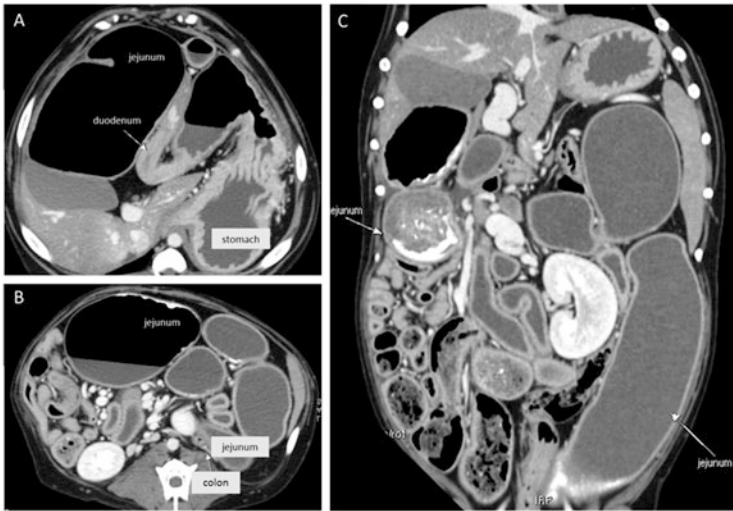

Fig. 27 Pseudo-obstruction in a dog with intestinal leiomyositis. (**a**, **b**) Transverse views of the abdomen showing multiple dilated, fluid-filled intestinal loops. (**c**) Dorsal MPR view showing intestinal distension in the absence of mechanical obstructive causes (consistent with functional ileus)

(adenocarcinoma and other subtypes) are the most common *gastric tumors* in dogs, accounting for 50–90% of cases, followed by leiomyosarcomas and lymphoma (Figs. 1, 5, 13, 17c, 18, and 29). The Tervuren, Bouvier des Flandres, Groenendael, Collie, standard Poodle, and Norwegian Elkhound breeds have been found to have a
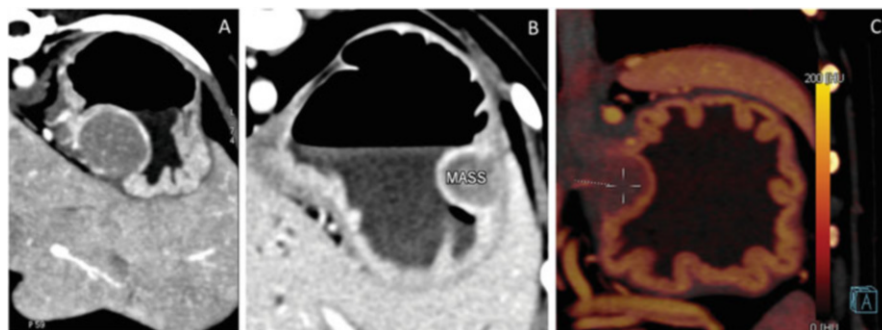
Fig. 28 Benign gastric tumors in dogs. Nodular eccentric lesions covered by intact mucosa. (**a**, **b**) Leiomyomas. (**c**) Adenoma (color-coded iodine map of dual-energy series)
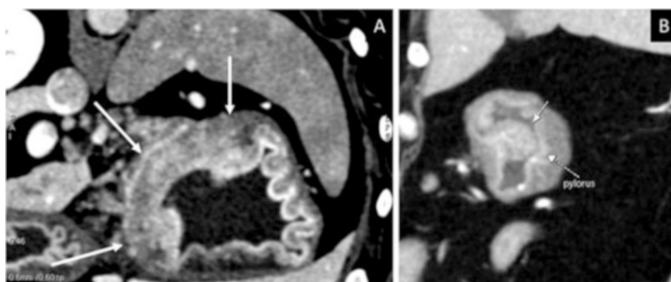

Fig. 29 Gastric carcinomas. (**a**) Eccentric thickening of the gastric wall. The rugal folds are not visible and the mucosa is disrupted. (**b**) Polypoid aspect of pyloric adenocarcinoma, partially obstructing the gastric outflow, in a dog

significantly increased risk of gastric carcinoma. Lymphosarcoma (isolated or as part of a more diffuse gastrointestinal tumor) is the most commonly reported primary gastric tumor in cats. It has a diverse array of appearances, ranging from infiltrative to polypoid lesions. Gastric adenocarcinomas are rare in cats. Extramedullary plasmacytomas have been described as primary gastric or bowel tumors in dogs and cats. Primary histiocytic sarcoma of the stomach has also been documented in dogs.

Adenocarcinoma and lymphosarcoma are the most common *intestinal tumors* in dogs and cats. Other bowel tumor types include leiomyomas, leiomyosarcomas, gastrointestinal stromal tumors, plasma cell tumors, mast cell tumors, carcinoids (tumors of neuroendocrine origin), and extraskeletal osteosarcomas (Figs. 8b, c, 9, 20c, 30, 31, and 32). Active gastrointestinal hemorrhage can accompany gastrointestinal cancer with mucosal ulceration, as well as benign ulcers (Fig. 1). Benign polyps and adenomas can be found in the feline duodenum and canine rectum. The
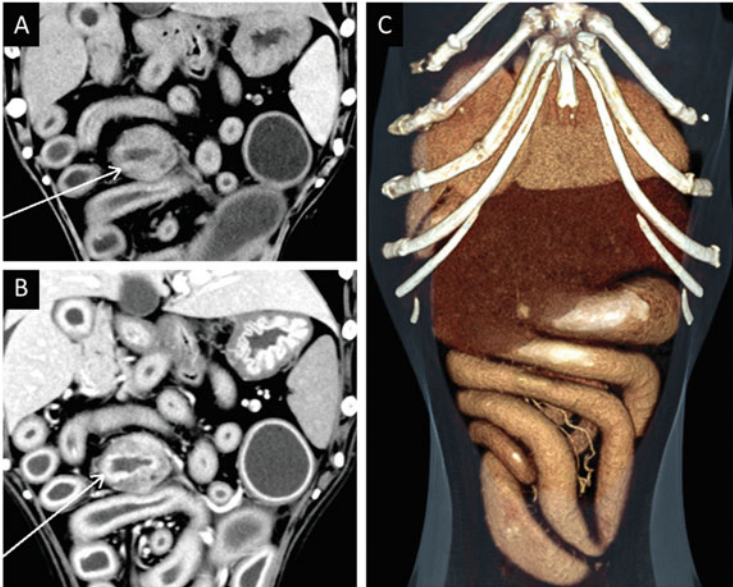
Fig. 30 Intestinal carcinoma in a dog. (**a**, **b**) Dorsal MPR views of the abdomen showing segmental thickening of the ileum (*arrow*). (**c**) Other intestinal loops are distended by fluid
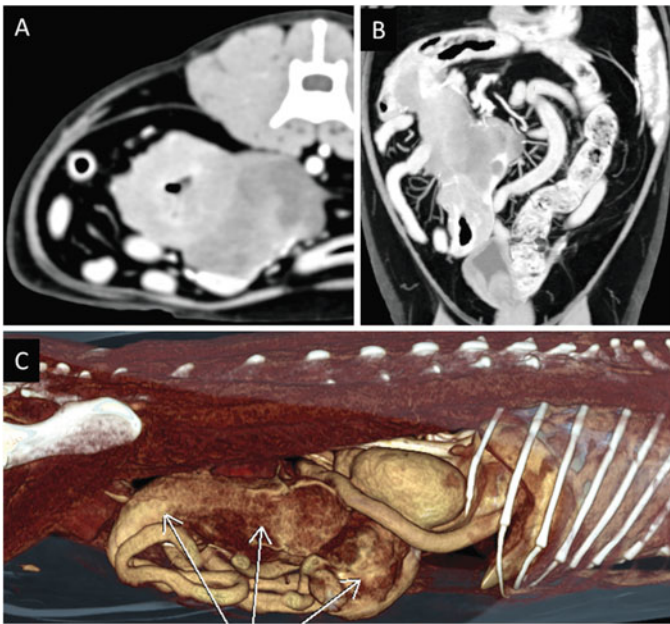
Fig. 31 Intestinal lymphoma in a cat. (**a**) Transverse view showing marked intestinal wall thickening, perilesional omental infiltration, and regional lymph node enlargement. (**b**, **c**) Dorsal MPR and right lateral volume-rendered images show the extension of the intestinal mass
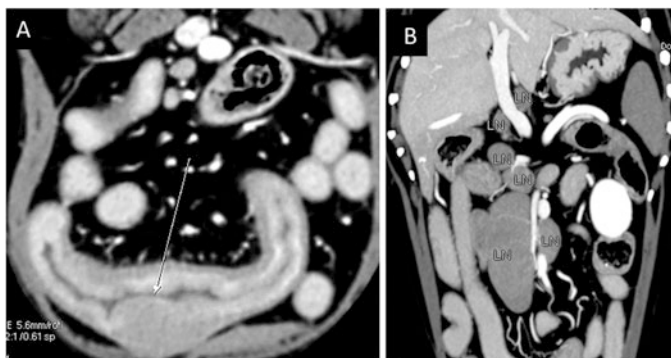
Fig. 32 Intestinal mastocytoma in a dog. (**a**) Transverse view showing segmental, eccentric intestinal thickening. (**b**) Dorsal MPR view of the same dog, showing marked enlargement of the regional lymph nodes (metastasis)
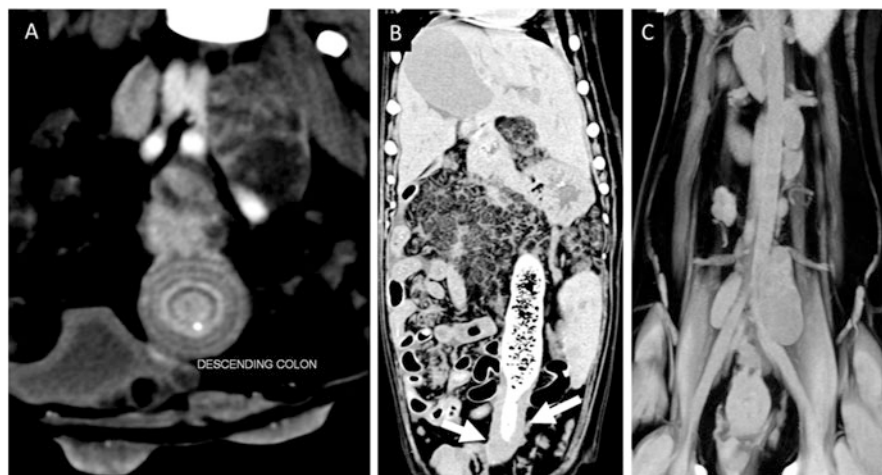
Fig. 33 Colon carcinoma in a dog. (**a**) Transverse view through the pelvis, showing the colon obstruction with a "target sign" appearance. (**b**) Dorsal MPR view showing colic wall thickening (*arrows*) and stenosis. Note the reticulonodular pattern of the peritoneum (carcinomatosis). (**c**) Dorsal MPR view of the retroperitoneal region shows secondary lymph node involvement (metastasis)

absence of mesenteric change and metastasis aids the diagnosis and rules out most malignancies. Malignant tumors of the rectum may show local infiltration, and the definition of the tumoral boundaries based on MDCT images only may be difficult (Figs. 14, 25, 33, 34).
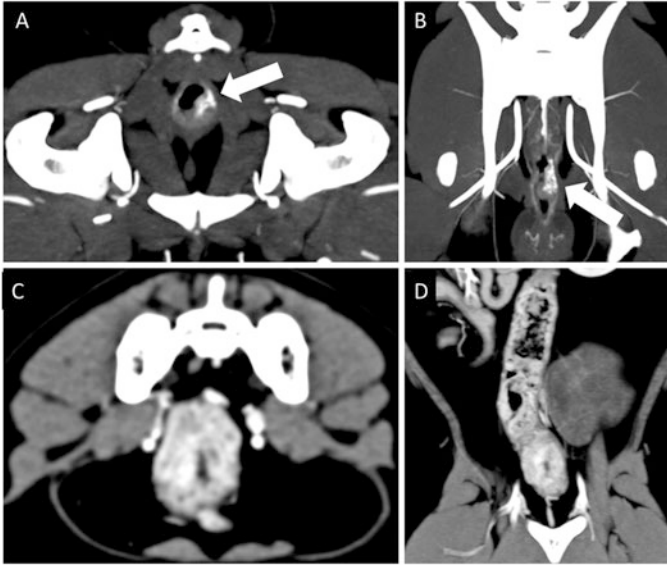
Fig. 34 Colon and rectal carcinomas. (**a**, **b**) Transverse and dorsal MPR views of the pelvis in a dog with small rectal carcinoma. Note the small hypervascular eccentric lesion (*arrow*). (**c**, **d**) Transverse and dorsal MPR images of the pelvis in a cat, showing circumferential wall thickening in the distal colon with marked post-contrast enhancement

Further Readings

Applewhite A, Cornell K, Selcer B. Pylorogastric intussusception in the dog: a case report and literature review. J Am Anim Hosp Assoc. 2001;37:238–43.

Bertolini G, Prokop M. Multidetector-row computed tomography: technical basics and preliminary clinical applications in small animals. Vet J. 2011;189(1):15–26. doi:10.1016/j.tvjl.2010.06.004.

Drost WT, Green EM, Zekas LJ, Aarnes TK, Su L, Habing GG. Comparison of computed tomography and abdominal radiography for detection of canine mechanical intestinal obstruction. Vet Radiol Ultrasound. 2016;57(4):366–75. doi:10.1111/vru.12353.

Fant P, Caldin M, Furlanello T, De Lorenzi D, Bertolini G, Bettini G, Morini M, Masserdotti C. Primary gastric histiocytic sarcoma in a dog – a case report. J Vet Med A Physiol Pathol Clin Med. 2004;51:358–62.

Fields EL, Robertson ID, Osborne JA, Brown JC Jr. Comparison of abdominal computed tomography and abdominal ultrasound in sedated dogs. Vet Radiol Ultrasound. 2012a;53(5):513–7. doi:10.1111/j.1740-8261.2012.01949.x.

Fields EL, Robertson ID, Brown JC Jr. Optimization of contrast-enhanced multidetector abdominal computed tomography in sedated canine patients. Vet Radiol Ultrasound. 2012b;53(5):507–12. doi:10.1111/j.1740-8261.2012.01950.x.

Fitzgerald E, Lam R, Drees R. Improving conspicuity of the canine gastrointestinal wall using dual phase contrast-enhanced computed tomography: a retrospective cross-sectional study. Vet Radiol Ultrasound. 2017 Jan 5. doi:10.1111/vru.12467.

Hoey S, Drees R, Hetzel S. Evaluation of the gastrointestinal tract in dogs using computed tomography. Vet Radiol Ultrasound. 2013;54(1):25–30. doi:10.1111/j.1740-8261.2012.01969.x.

Rivero MA, Vázquez JM, Gil F, Ramírez JA, Vilar JM, De Miguel A, Arencibia A. CT-soft tissue window of the cranial abdomen in clinically normal dogs: an anatomical description using macroscopic cross-sections with vascular injection. Anat Histol Embryol. 2009;38(1):18–22. doi:10.1111/j.1439-0264.2008.00886.x.

Seim-Wikse T, Jörundsson E, Nødtvedt A, et al. Breed predisposition to canine gastric carcinoma – a study based on the Norwegian canine cancer register. Acta Vet Scand. 2013;55(1):25. doi:10.1186/1751-0147-55-25.

Shanaman MM, Hartman SK, O'Brien RT. Feasibility for using dual-phase contrast-enhanced multi-detector helical computed tomography to evaluate awake and sedated dogs with acute abdominal signs. Vet Radiol Ultrasound. 2012;53(6):605–12. doi:10.1111/j.1740-8261.2012.01973.x.

Shanaman MM, Schwarz T, Gal A, O'Brien RT. Comparison between survey radiography, B-mode ultrasonography, contrast-enhanced ultrasonography and contrast-enhanced multi-detector computed tomography findings in dogs with acute abdominal signs. Vet Radiol Ultrasound. 2013;54(6):591–604. doi:10.1111/vru.12079.

Teixeira M, Gil F, Vazquez JM, Cardoso L, Arencibia A, Ramirez-Zarzosa G, Agut A. Helical computed tomographic anatomy of the canine abdomen. Vet J. 2007;174(1):133–8.

Terragni R, Vignoli M, Rossi F, Laganga P, Leone VF, Graham JP, Russo M, Saunders JH. Stomach wall evaluation using helical hydro-computed tomography. Vet Radiol Ultrasound. 2012;53(4):402–5. doi:10.1111/j.1740-8261.2012.01928.x.

Yamada K, Morimoto M, Kishimoto M, Wisner ER. Virtual endoscopy of dogs using multi-detector row CT. Vet Radiol Ultrasound. 2007;48(4):318–22.

Zacuto AC, Pesavento PA, Hill S, McAlister A, Rosenthal K, Cherbinsky O, Marks SL. Intestinal leiomyositis: a cause of chronic intestinal pseudo-obstruction in 6 dogs. J Vet Intern Med. 2016;30(1):132–40. doi:10.1111/jvim.13652. Epub 2015 Nov 26.